Received: 15 September 2020 | Revised: 8 January 2021 | Accepted: 1 February 2021

IET Communications

DOI: 10.1049/cmu2.12142

The Institution of Engineering and Technology WILEY

ORIGINAL RESEARCH PAPER

Relay selection for spatially random full-duplex cooperative non-orthogonal multiple access networks

Xinyu Wang[1,2] | **Min Jia**[1] | **Ivan Wang-Hei Ho**[2] | **Qing Guo**[1] | **Francis Chung-Ming Lau**[2]

[1] School of Electronics and Information Engineering, Harbin Institute of Technology, Harbin, Heilongjiang, China

[2] Department of Electronic and Information Engineering, The Hong Kong Polytechnic University, Hong Kong, SAR, China

Correspondence
Min Jia, School of Electronics and Information Engineering, Harbin Institute of Technology, Harbin, Heilongjiang 150080, China.
Email: jiamin@hit.edu.cn

Funding information
Natural Science Foundation for Outstanding Young Scholars of Heilongjiang Province, Grant/Award Number: YQ2020F001; National Natural Science Foundation of China, Grant/Award Number: 61771163; The Hong Kong Polytechnic University Projects, Grant/Award Numbers: G-YBK6, G-YBR2; Science and Technology on Communication Networks Laboratory, Grant/Award Number: SXX19641X072; General Research Fund established under the University Grant Committee of the Hong Kong Special Administrative Region, China, Grant/Award Number: 15201118

Abstract

This paper investigates the relay selection problem and proposes a three-stage relay selection strategy with power allocation (TRSPA) for a spectrum-sensing-based full-duplex (FD) user relaying cooperative non-orthogonal multiple access (CNOMA) scheme. Uniformly-distributed strong user relays in the investigated scheme help a weak user communicates with the base station in an efficient and reliable way. The proposed TRSPA strategy maximizes the transmission data rate of the selected relay while ensuring successful transmissions for the weak user by precisely narrowing down relay candidates step-by-step and dynamically allocating optimal power coefficients. Exact and asymptotic outage probabilities and ergodic rates are worked out. Accordingly, diversity orders and spatial multiplexing gains are derived. We further exploit the impact of self-interference (SI) on TRSPA for FD-CNOMA and then compare its performance with TRSPA applied in other relaying modes, that is half-duplex and orthogonal multiple access. Finally, simulation results reveal that: (i) theoretical derivation results are correct; (ii) TRSPA always outperforms other relay selection strategies in terms of outage probability and ergodic rate; and (iii) TRSPA for FD-CNOMA in a real-world scenario achieves better performance than other relaying modes in spite of the adverse effect of SI in FD mode.

1 | INTRODUCTION

With the rapid advancement in the Internet of Things and the mobile communication networks, enormous amounts of wireless connections and dramatically increasing mobile data traffic are emerging [1, 2]. Considering limited wireless resources, conventional orthogonal multiple access (OMA) can hardly cope with such overwhelming development trends due to the insufficient utilization of spectrum resources caused by the following inherent features of real-time machine type communication devices (MTCDs). (i) Transmissions are generally infrequent with large inter-arrival time [3]. Spectrum resources are wasted when MTCDs finish transmissions and stop occupying the spectrum bands. (ii) The target transmission rate of a MTCD is fixed [3] and relatively low [4]. Even if the MTCD occupies the spectrum band, the spectrum efficiency is still quite small and the spectrum resource is actually underutilized. Therefore, a novel access method with a significant improvement in resource utilization efficiency is in great demand.

To solve the above wastage issues, spectrum sensing and non-orthogonal multiple access (NOMA) [5] techniques are adopted in an access method proposed in [6]. The proposed method is a cooperative NOMA (CNOMA) [7, 8] scheme, where a strong

user with good channel conditions works as a full-duplex (FD) relay to assist another user with weak channel conditions to forward its signals by transmitting a superimposed NOMA signal consisting of messages from both users to the base station (BS). The BS then decodes the NOMA signal according to the successive interference cancellation (SIC) protocol [9]. In this way, each spectrum band is shared by multiple users with good and bad channel conditions. The corresponding spectrum efficiency is therefore increased compared with the traditional OMA scheme where each spectrum band is completely occupied by the weak user alone [5]. Thus, the above-mentioned wastage issue of under-utilized spectrum resource is solved. Moreover, FD-CNOMA requires the user relay to identify unoccupied spectrum resources for signal transmissions by spectrum sensing. In this way, the wastage issue of idle spectrum resources is avoided. Considering additional time resource costs of the half-duplex (HD) mode caused by alternatively receiving and transmitting, FD mode is employed. FD has the potential to yield higher data transmission rate than HD. We only have one concern about FD, that is self-interference (SI). Thanks to the rapidly developing SI suppression techniques [10], there is a strong possibility for realizing the advantages of FD mode. We will insightfully discuss the impact of SI on FD later.

1.1 | Motivation

This paper investigates relay selection (RS) for FD-CNOMA. RS research contributions mainly include two categories based on the relaying mode adopted by relays, namely HD and FD. Ding et al. proposed a RS strategy for a CNOMA system to achieve the minimal overall outage probability [11]. Yang et al. considered the unicast traffic where one BS communicated with two mobile users with the aid of multiple dedicated relays [12]. Two kinds of RS strategies for CNOMA networks with decode-and-forward and amplify-and-forward relaying protocols were proposed, respectively. For a multicast cognitive CNOMA system, Lv et al. presented three different secondary user scheduling strategies based on the available channel state information (CSI) to exploit the inherent spatial diversity [13]. Xu et al. investigated optimal RS schemes for CNOMA networks with multiple dedicated relays by adaptively ordering users based on instantaneous CSI rather than quality of service (QoS) requirements [14]. Related works [11–14] are all based on HD relaying. These achievements have laid a solid foundation for the understanding of RS strategies for HD-CNOMA. However, the improvement of reliability and capacity comes at the price of resource utilization efficiency reduction due to the additional time resource cost during HD cooperation [15], which may offset the capacity gain promised by cooperation communication. In contrast, FD mode is capable of overcoming the capacity loss in HD-CNOMA systems since FD wireless device transmits and receives simultaneously [16]. But RS for FD relaying CNOMA is far from being well studied. The only relevant finding was presented in [4]. Yue et al. investigated the impact of RS on the performance of CNOMA, where relays were capable of working in either FD or HD mode [4]. In their proposed RS scheme, on the condition of ensuring the data rate of distant user, they served the nearby user with data rate as large as possible for selecting a relay. However, their proposed RS scheme has the following two drawbacks. Firstly, a fixed power allocation was used by [4]. Optimizing the power allocation coefficients based on CSI will further improve the performance of CNOMA [13]. To the best of our knowledge, there are no existing works investigating a dynamic power-allocation-based RS scheme for CNOMA networks with FD relays. Secondly, the RS scheme presented in [4] is a centralized system. Channel estimation, relay selection and relevant data processing are controlled and completed by the BS itself, leading to a large demand of control signalling and system overhead.

Additionally, a general conclusion of research findings about CNOMA, such as [4, 17, 18] and [19], is that FD relaying CNOMA is superior to HD-based CNOMA in the low signal-to-noise ratio (SNR) region but not in the high SNR region due to effects of residual SI. However, this conclusion still lacks a clear and explicit guidance to choose which relaying mode in practice. This is another focus of this paper.

1.2 | Contribution

Motivated by Section 1.1, we take a further step and propose a three-stage RS strategy with dynamic power allocation (TRSPA) for the FD-CNOMA scheme to overcome the two drawbacks of [4].

Due to the limited transmission capability [20] and the possible severe fading effect caused by physical obstacles or remote cell-edge location, a MTCD is regarded as the weak user and it desires the assistance from other user relays. Real-time MTCDs are sensitive to time delay and they have the priority to access spectrum bands [3] to satisfy their QoS requirements first. In contrast, cellular user relays are not sensitive to time delay, which makes them suitable to access a spectrum band opportunistically when the QoS requirements of real-time MTCDs are met. Thus, the purpose of our proposed relay selection strategy TRSPA is to find out the best user relay to maximize the ergodic rate of that selected relay on the condition of guaranteeing successful transmissions of the MTCD's signal.

During the first stage of TRSPA, each relay senses the spectrum band to determine whether MTCD exists or not and then relays with positive sensing results further decode MTCD's signal. The first stage guarantees successful transmissions of the MTCD's signal to the user relay candidates. The second stage aims to further ensure the MTCD's successful transmissions from remaining relay candidates to the BS. In the third stage, the best relay is selected from remaining candidates and in the meanwhile, power allocation coefficients are determined according to instantaneous CSI to realize the optimization purpose of TRSPA. Different from [4] with fixed power allocations, power allocation coefficients adopted by our proposed

TRSPA scheme are dynamically adjusted to optimal values all the time, in order to maximize the ergodic rate of the selected user relay and to realize successful transmissions of the MTCD's signal. Relevant proofs will be presented in our paper to illustrate these power allocation coefficients are indeed the optimal results. Furthermore, different from [4], the system considered in our paper is in fact a distributed system. Signal detection and decoding, power allocation, and relay selection are entirely completed by relays, instead of the BS. The role of the BS in our considered system model is merely a receiver, but not a controller. This kind of distributed system is more flexible and efficient with less control signalling and system overhead compared with the centralized system presented by [4].

Finally, we also reveal the practical impact of SI on TRSPA for FD-CNOMA in terms of outage probability and ergodic rate.

The major contributions of this paper are summarized as follows.

- We investigate a three-stage RS strategy for a FD-CNOMA scheme with spectrum sensing. With a dynamic power allocation method, TRSPA is proved to achieve the optimal outage probability and on this basis, the largest ergodic rate, among all possible RS strategies.
- We characterize the performance of TRSPA for FD-CNOMA with imperfect SI cancellation. We derive the closed-form expressions of outage probability and ergodic rate. From the standpoint of practicality, relays are modelled as uniformly distributed. Also, we confirm that the diversity order of the weak user is worked out to be zero due to the effects of residual SI. The spatial multiplexing gain of strong user relay is worked out to be one, which is its achievable maximum value.
- Different from the inexplicit conclusion of other works, we straightforwardly reveal that even with the adverse effects of SI, FD-CNOMA with reasonable SI suppression capabilities still achieves superior performance over HD-CNOMA and cooperative OMA (COMA). We confirm that FD is the most sensible choice when designing a TRSPA strategy in reality.

The main notations are shown as follows: $E(\cdot)$ denotes the expectation operation; $\log(\cdot)$, $\lg(\cdot)$, and $\ln(\cdot)$ denote the base-2, base-10, and natural logarithmic functions, respectively.

The rest of this paper is organized as follows. In Section 2, we describe the network model of the considered FD relaying CNOMA scenario. Section 3 presents the performance evaluation results of the proposed relay selection strategy TRSPA in terms of outage probability and ergodic rate. Accordingly, diversity orders and spatial multiplexing gains are derived. Next, Section 4 further exploits the impact of SI on TRSPA for FD-CNOMA and then compares its performance with TRSPA applied in other relaying modes, namely HD and OMA. Section 5 provides numerical simulation results to validate theoretical derivation results and to illustrate the superior performance of the proposed relay selection strategy compared to other RS strategies and other relaying modes. Finally, Section 6 gives some concluding remarks.

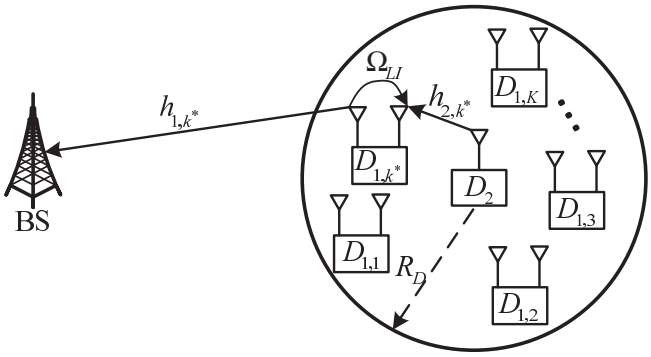

FIGURE 1 System model

2 | NETWORK MODEL

2.1 | Network description

We consider a FD relaying CNOMA scenario consisting of one BS, K FD user relays ($D_{1,k}$ with $1 \le k \le K$) and one user (D_2), in the uplink communication system as shown in Figure 1. $\mathcal{S}$ denotes the set of relays in the network. The relays are equipped with two antennas, one for reception and one for transmission, while all other nodes are equipped with a single antenna. Like [18] and [21], this paper assumes there does not exist any direct link between the BS and the weak user D_2 because of D_2's limited transmission capability [20] and the severe shadowing effects caused by physical obstacles. In such case, D_2 cannot upload signals to the BS all by itself, which is the main reason why it desires the assistance of a selected relay D_{1,k^*} ($D_{1,k^*} \in \mathcal{S}$) by our proposed relay selection strategy TRSPA in Section 2.3. User relays that are not selected will send their respective messages to the BS using resource blocks other than the one occupied by D_2 and D_{1,k^*}, which is the same with a traditional OMA scheme. Therefore, we only focus on the performance of D_2 and D_{1,k^*}. We assume that D_2 is located at the origin of a disc with a radius of R_D. K relays are uniformly distributed in that disc. Wireless links are assumed to follow independent non-selective block Rayleigh fading [22–27] and are corrupted by additive white Gaussian noise with a power value of N_0. $h_{1,k} = \frac{h}{\sqrt{1+d_{1,k}^{\alpha}}}$ and $h_{2,k} = \frac{h'}{\sqrt{1+r_{2,k}^{\alpha}}}$ [4], respectively, represent the channel coefficients of $D_{1,k} \to$ BS and $D_2 \to D_{1,k}$ links, where $d_{1,k}$ is the distance between $D_{1,k}$ and the BS, and $r_{2,k}$ is the distance between D_2 and $D_{1,k}$. h and h' are independent Rayleigh fading channel gains and α represents the path loss exponent. We assume that $d_{1,k} \gg r_{2,k}$ [4]. Moreover, $d_{1,k} = \sqrt{d_{D_2,BS}^2 + r_{2,k}^2 - 2d_{D_2,BS}r_{2,k}\cos(\theta_k)}$, where $d_{D_2,BS}$ is the distance between D_2 and the BS and θ_k denotes the angle $\angle D_{1,k}D_2$ BS. For the sake of practicality, we assume that residual loop self-interference (LI) exists at $D_{1,k}$. The LI signal is assumed to be additive Gaussian signal with zero mean [6, 28]. The assumption of a Gaussian distribution might hold in reality because of the various sources of imperfections in the cancellation process based on the central limit theorem. Moreover, the

variance of this Gaussian LI signal is $\Omega_{LI}P_r$ based on [10] and [29], where P_r is the normalized transmit power of each relay and Ω_{LI} is its LI cancellation coefficient. $x_{1,k}$ and x_2 are messages transmitted by $D_{1,k}$ and D_2. We consider the case that $x_{1,k}$ and x_2 form a NOMA group, as the two-user NOMA case is reasonably followed in [4, 13, 17–19] and [21]. Such case is also investigated in the Third Generation Partnership Project. In fact, the subsequent analysis can be extended for a multiple-user scenario by clustering.

To prepare for the proposal of TRSPA, we take an arbitrary user relay $D_{1,k}$ as an example to describe how a user relay assists D_2 in the FD-CNOMA scheme presented in Figure 1. D_2 appears and disappears randomly. $D_{1,k}$ detects the received signal and determines whether D_2 exists or not. If $D_{1,k}$'s detection result shows the existence of D_2, $D_{1,k}$ will then try to decode x_2. After $D_{1,k}$ has successfully obtained x_2, $D_{1,k}$ transmits a superimposed NOMA signal consisting of x_2 and $x_{1,k}$ to the BS. Based on SIC [9], the BS will successively decode messages of D_2 and $D_{1,k}$. Otherwise, if the detection result claims D_2 does not exist, $D_{1,k}$ will directly transmit its own message using full power. BS then directly decodes $x_{1,k}$.

2.2 | Signal model

The signal received by $D_{1,k}$ is $y^r_{D_{1,k}}[l] = \begin{cases} \sqrt{P_s}h_{2,k}x_2[l] + \varpi_1 x_{LI,k}[l] + n_{D_{1,k}}[l], & H_1 \\ \varpi_1 x_{LI,k}[l] + n_{D_{1,k}}[l], & H_0 \end{cases}$, where $x_{LI,k}$ denotes the LI signal at $D_{1,k}$ and $n_{D_{1,k}}$ is the noise signal, during the l-th time slot. P_s is the normalized transmit power of D_2. In the following analysis, we assume that $P_r = P_s$[1] [17–19, 21]. H_1 and H_0 refer to the hypotheses that D_2 exists or not, respectively. ϖ_1 is an indicator variable, where $\varpi_1 = 1$ denotes the relay working in FD mode. For comparison, we will also study HD and OMA modes where $\varpi_1 = 0$.

Recalling the FD-CNOMA scheme illustrated in Section 2.1, if $D_{1,k}$ claims the existence of D_2, $D_{1,k}$ will decode x_2 from its received signal with the signal-to-interference-plus-noise ratio (SINR) of

$$\gamma_{D_2\to D_{1,k}} = \frac{|h_{2,k}|^2\rho}{\varpi_1\Omega_{LI}\rho + 1}, \tag{1}$$

where $\frac{P_r}{N_0} = \frac{P_s}{N_0} \triangleq \rho$ is the transmit SNR. We first consider the case that $D_{1,k}$ correctly decodes D_2. $D_{1,k}$ transmits the superimposed NOMA signal $y^t_{D_{1,k}}[l] = \sqrt{P_r a_{1,k}}x_{1,k}[l] + \sqrt{P_r a_{2,k}}x_2[l-\tau]$, where τ represents the processing delay at $D_{1,k}$ with an integer $\tau \geq 1$. $a_{1,k}$ and $a_{2,k}$ are power allocation coefficients for $x_{1,k}$ and x_2, respectively, where $a_{1,k} + a_{2,k} = 1$. The received signal at the BS is $y^r_{BS}[l] = h_{1,k}y^t_{D_{1,k}}[l] + n_{BS}[l]$, where n_{BS} denotes the noise signal at the BS. Similar to [4, 11] and [13], D_2 and $D_{1,k}$ are sorted based on their QoS priority during SIC. D_2 should access the spectrum band with a high priority, as discussed in Section 1. Therefore, during SIC, the BS first decodes x_2 with the SINR value of

$$\gamma_{D_2\to D_{1,k}\to BS} = \frac{a_{2,k}|h_{1,k}|^2\rho}{a_{1,k}|h_{1,k}|^2\rho + 1}. \tag{2}$$

After decoding x_2 and subtracting it from y^r_{BS}, the BS will decode $x_{1,k}$ with a SNR value of

$$\gamma_{D_{1,k}\to BS} = a_{1,k}|h_{1,k}|^2\rho. \tag{3}$$

We then consider the case that $D_{1,k}$ fails to detect and obtain x_2. It will directly send its own message to the BS with full power so that the power resource is sufficiently utilized. Under such condition, the received SNR value at the BS when it decodes $x_{1,k}$ is given by

$$\hat{\gamma}_{D_{1,k}\to BS} = |h_{1,k}|^2\rho. \tag{4}$$

2.3 | Relay selection strategy

In this subsection, both our proposed TRSPA strategy and other relay selection benchmarks with various relaying modes are presented to prepare for subsequent comparison.

2.3.1 | Three-stage relay selection with power allocation

In the first stage, all relays sense the spectrum band to determine whether D_2 exists or not and then relays with positive sensing results further decode x_2. Therefore, the following subset $\mathcal{S}_1$ ($\mathcal{S}_1 \subseteq \mathcal{S}$) is built.

$$\mathcal{S}_1 = \Big\{D_{1,k} : 1 \leq k \leq K, \; T_{ED,k} \geq \lambda, \; \log\left(1 + \gamma_{D_2\to D_{1,k}}\right) \geq R_2\Big\}, \tag{5}$$

where R_2 is the target data rate of x_2; $T_{ED,k} = \frac{1}{L}\sum_{l=1}^{L}\left(y^r_{D_{1,k}}[l]\right)^2$ represents the test statistic of energy detection (ED) by $D_{1,k}$; L represents the sampling number; λ is the detection threshold of ED, which is determined by the preset false alarm probability P_f^{pre}. As stated in [6], FD-CNOMA adopts the widely used ED, since it is efficient and simple to be implemented in hardware.

In the second stage, we intend to find out all relays within $\mathcal{S}_1$ which are able to successfully forward x_2 to the BS. If the BS fails to decode x_2 even when $a_{1,k} = 0$, then the corresponding $D_{1,k}$ will by no means succeed. Therefore, we substitute $a_{1,k} = 0$ into (2) and get the maximum value of $\gamma_{D_2\to D_{1,k}\to BS}$, that is $\gamma_{D_2\to D_{1,k}\to BS,MAX} = |h_{1,k}|^2\rho$. As long as $\log(1 + |h_{1,k}|^2\rho) \geq$

[1] This is assumed to simplify the derivation process. A similar technique can be applied when $P_r \neq P_s$.

R_2, $D_{1,k}$ is likely to realize the successful transmission of x_2. In conclusion, the second stage is to build the following subset $\mathcal{S}_2$ ($\mathcal{S}_2 \subseteq \mathcal{S}_1$) to enable the BS to decode x_2 correctly.

$$\mathcal{S}_2 = \left\{ D_{1,k} : \ D_{1,k} \in \mathcal{S}_1, \ \log\left(1 + \left|h_{1,k}\right|^2 \rho\right) \geq R_2 \right\}. \quad (6)$$

For the third stage, we select the relay D_{1,k^*} by (7).

$$k^* = \underset{k \in \{1,2,\ldots,K\}}{\arg} \max \left|h_{1,k}\right|^2 \quad \text{s.t.} \quad D_{1,k} \in \mathcal{S}_2. \quad (7)$$

According to [13], the relay with maximum $|h_{1,k}|^2$ can be found out by a virtual timer. Each relay $D_{1,k}$ ($D_{1,k} \in \mathcal{S}_2$) starts a virtual timer initiated by $t_n = t_0 \exp(-|h_{1,k}|^2)$, where t_0 is a constant. The timer of $D_{1,k}$ with the best channel condition to the BS (i.e. the selected relay D_{1,k^*}) will expire first. Then D_{1,k^*} broadcasts a flag message signalling its presence and other relays back off. Moreover, the optimal power allocation coefficient is dynamically worked out based on CSI as shown in (8).

$$a_{1,k} = \frac{\left|h_{1,k}\right|^2 \rho - T_2}{\left|h_{1,k}\right|^2 \rho (1 + T_2)}, \quad (8)$$

where $T_2 = 2^{R_2} - 1$ is the target SNR when decoding x_2. The purpose of our proposed relay selection strategy TRSPA is to find out the best user relay in order to maximize the ergodic rate of that selected relay on the condition of guaranteeing successful transmissions of D_2's signal, which means x_2 is successfully decoded by the BS. Here we claim that the power allocation coefficient given by (8) is optimal and relevant proofs will be presented in Theorem 1 and Theorem 2 by illustrating (8) indeed enables TRSPA to achieve that goal.

It is noted that if $|\mathcal{S}_1| = 0$ or $|\mathcal{S}_2| = 0$, where $|\mathcal{S}_1|$ and $|\mathcal{S}_2|$ refer to the sizes of $\mathcal{S}_1$ and $\mathcal{S}_2$, respectively, it is impossible for any relay to realize the successful transmission of x_2. Similar to the case of (4), relays will then directly transmit their own messages with full power. In order to achieve the largest data transmission rate, the selected relay is given by

$$\begin{aligned} k^* &= \underset{k \in \{12\cdots K\}}{\arg} \max \hat{\gamma}_{D_{1,k} \to BS} \text{ s.t. } D_{1,k} \in \mathcal{S} \\ &= \underset{k \in \{12\cdots K\}}{\arg} \max \left|h_{1,k}\right|^2 \text{ s.t. } D_{1,k} \in \mathcal{S}. \end{aligned} \quad (9)$$

Theorem 1. *For a FD-CNOMA scheme, the power allocation coefficient given by (8) enables the proposed TRSPA strategy to minimize the outage probability of D_2.*

Proof. As above-stated, the premise is to ensure successful transmissions of D_2's signal. Therefore, in this proof, we aim to illustrate that with the power allocation coefficient given by (8), our proposed TRSPA scheme achieves the optimal outage performance, that is $D_{1,\tilde{k}}$ with a channel coefficient of $h_{1,\tilde{k}}$ between itself and the BS is chosen by any other RS strategy with power coefficients $a_{1,\tilde{k}}$ and $a_{2,\tilde{k}}$. If x_2 is successfully decoded by the BS with the assistance of $D_{1,\tilde{k}}$, then $\frac{a_{2,\tilde{k}}|h_{1,\tilde{k}}|^2\rho}{a_{1,\tilde{k}}|h_{1,\tilde{k}}|^2\rho+1} \geq T_2$ must be true based on (2). We also learn that $|\mathcal{S}_1| \neq 0$, since at least $D_{1,\tilde{k}}$ obtains x_2. Moreover, based on $\frac{a_{2,\tilde{k}}|h_{1,\tilde{k}}|^2\rho}{a_{1,\tilde{k}}|h_{1,\tilde{k}}|^2\rho+1} \geq T_2$, we have $0 \leq a_{1,\tilde{k}}|h_{1,\tilde{k}}|^2\rho \leq \frac{|h_{1,\tilde{k}}|^2\rho - T_2}{1+T_2}$, which means $T_2 \leq |h_{1,\tilde{k}}|^2\rho$. Thus, $D_{1,\tilde{k}} \in \mathcal{S}_2$ according to (6) and we get $|\mathcal{S}_2| \neq 0$. Since $|\mathcal{S}_1| \neq 0$ and $|\mathcal{S}_2| \neq 0$, the selected relay by TRSPA is $k^* = \underset{k \in \{1,2,\ldots,K\}}{\arg} \max |h_{1,k}|^2$ s.t. $D_{1,k} \in \mathcal{S}_2$ and the corresponding power coefficient is $a_{1,k^*} = \frac{|h_{1,k^*}|^2\rho - T_2}{|h_{1,k^*}|^2\rho(1+T_2)}$ based on (7) and (8). In such case, $\gamma_{D_2 \to D_{1,k} \to BS} = \frac{a_{2,k^*}|h_{1,k^*}|^2\rho}{a_{1,k^*}|h_{1,k^*}|^2\rho+1} = T_2$, which means x_2 can also be correctly decoded by the BS with the assistance of the selected D_{1,k^*} by our proposed TRSPA strategy. In conclusion, as long as there exists any RS strategy with any power allocation coefficient, which realizes successful decoding, our proposed TRSPA will be capable of doing so as well. Therefore, our proposed power allocation method (8) enables TRSPA to realize the smallest outage probability among all possible relay selection strategies with any possible power allocation coefficient. In other words, from the perspective of outage performance for D_2, the power allocation coefficient (8) is proved to be optimal, which completes the proof. □

Theorem 2. *The power allocation coefficient given by (8) enables the proposed TRSPA to achieve the largest ergodic rate for the selected user relay when x_2 is successfully decoded by the BS.*

Proof. As above-stated, our purpose is to find out the best user relay to maximize its ergodic rate on the condition of guaranteeing successful transmissions of D_2's signal. Therefore, in this proof, we aim to illustrate that with the power allocation coefficient given by (8), our proposed TRSPA scheme achieves the largest ergodic rate for the selected user relay when x_2 is successfully decoded by the BS.

We continue with the proof of Theorem 1. When x_2 is successfully decoded by the BS, we have $\frac{a_{2,\tilde{k}}|h_{1,\tilde{k}}|^2\rho}{a_{1,\tilde{k}}|h_{1,\tilde{k}}|^2\rho+1} \geq T_2$. Therefore, $a_{1,\tilde{k}}|h_{1,\tilde{k}}|^2\rho \leq \frac{|h_{1,\tilde{k}}|^2\rho - T_2}{1+T_2} \leq \frac{|h_{1,k}|^2_{MAX}\rho - T_2}{1+T_2}$, where $|h_{1,k}|^2_{MAX}$ represents the largest channel power gain among all relays within $\mathcal{S}_2$ ($|\mathcal{S}_2| \neq 0$ based on Theorem 1). According to (7) and (8), the selected relay by our proposed TRSPA strategy satisfies $a_{1,k^*}|h_{1,k^*}|^2\rho = \frac{|h_{1,k}|^2_{MAX}\rho - T_2}{1+T_2}$. Therefore, $\log(1 + a_{1,\tilde{k}}|h_{1,\tilde{k}}|^2\rho) \leq \log(1 + a_{1,k^*}|h_{1,k^*}|^2\rho)$, that is $\gamma_{D_{1,\tilde{k}} \to BS} \leq \gamma_{D_{1,k^*} \to BS}$. That is to say our proposed power allocation method (8) enables TRSPA to realize the largest ergodic rate of the selected relay among all possible relay selection strategies with any possible power allocation coefficient. In other words, from the perspective of ergodic rate for the selected user relay, the power allocation coefficient (8) is proved to be optimal, which completes the proof. □

In conclusion, the proposed power allocation coefficient (8) is proved to achieve the optimal outage performance, on which basis, the largest ergodic rate, among all possible methods. Considering the above-mentioned purpose of our relay selection strategy, (8) indeed enables the proposed TRSPA to maximize the ergodic rate of the selected relay on the condition of guaranteeing successful transmissions of D_2's signal. Therefore, the power allocation coefficient given by (8) is proved to be optimal.

2.3.2 | Max-min relay selection

$k^*_{Max-Min} = \arg\max_{k}\{\min[|h_{1,k}|^2, |h_{2,k}|^2] : D_{1,k} \in \mathcal{S}\}$ [30].

2.3.3 | Single-stage relay selection

Based on [4], single-stage relay selection (SRS) strategy chooses the relay $k^*_{SRS} = \arg\max_{k} \{\min[\log(1 + \frac{|h_{2,k}|^2\rho}{\varpi_1\Omega_{LI}\rho+1}), \log(1 + \frac{a^{SRS}_{2,k}|h_{1,k}|^2\rho}{a^{SRS}_{1,k}|h_{1,k}|^2\rho+1})]\}$, where $a^{SRS}_{1,k}$ and $a^{SRS}_{2,k}$ are the predefined power coefficients for the user relay and the weak user.

2.3.4 | Two-stage relay selection

According to the reference [11], Two-stage relay selection (TRS) first builds a subset $\mathcal{S}_{TRS} = \{D_{1,k} : 1 \le k \le K, \log(1 + \frac{|h_{2,k}|^2\rho}{\varpi_1\Omega_{LI}\rho+1}) \ge R_2, \log(1 + \frac{a^{TRS}_{2,k}|h_{1,k}|^2\rho}{a^{TRS}_{1,k}|h_{1,k}|^2\rho+1}) \ge R_2\}$, where $a^{TRS}_{1,k}$ and $a^{TRS}_{2,k}$ are the predefined power coefficients. For comparison fairness, we assume that relays in a TRS strategy also have the capability of spectrum sensing. Then the second stage is to select a relay $D_{1,k^*_{TRS}}$ within $\mathcal{S}_{TRS}$ where $k^*_{TRS} = \arg\max_{k}\{\log(1 + a^{TRS}_{1,k}|h_{1,k}|^2\rho) : D_{1,k} \in \mathcal{S}_{TRS}\}$.

2.3.5 | HD-CNOMA

The critical difference between the HD counterpart (i.e. HD-CNOMA) [31] and FD-CNOMA is whether user relays work in HD or FD relaying modes.

2.3.6 | COMA

Inspired by [17], the COMA counterpart is improved as follows for comparison fairness. In the first slot, the user relay determines whether D_2 exists or not by spectrum sensing. If the detection result claims the existence of D_2, the relay will decode x_2 and then successively transmit $x_{1,k}$ and x_2 in the next two slots. Otherwise, it will only transmit $x_{1,k}$ in the next two slots.

3 | ANALYTICAL PERFORMANCE EVALUATION

3.1 | Outage probability of D_2

3.1.1 | Outage probability of D_2 and diversity analysis under H_1

Denote φ_1 as the event that all relays fail to detect and decode x_2 correctively. If there exist some relays (e.g. j relays, $1 \le j \le K$) successfully obtaining x_2, we denote φ_2 as the event that none of them are capable of forwarding x_2 to the BS. The outage event of x_2 is then expressed as $\varphi = \varphi_1 \cup \varphi_2$, and thus the outage probability of D_2 for TRSPA in a FD-CNOMA scheme (i.e. TRSPA-FD) is

$$\begin{aligned} P^{TRSPA-FD}_{D_2} &= \Pr(\varphi_1) + \Pr(\varphi_2) = \Pr(|\mathcal{S}_1| = 0) \\ &\quad + \sum_{j=1}^{K} \Pr(|\mathcal{S}_2| = 0 | |\mathcal{S}_1| = j) = \left(1 - P^{FD}_{sd}\right)^K \\ &\quad + \sum_{j=1}^{K} C^j_K \left(P^{FD}_{sd}\right)^j \left(1 - P^{FD}_{sd}\right)^{K-j} \left(1 - J^{FD}_{d}\right)^j \\ &= \left(\left(1 - P^{FD}_{sd}\right) + P^{FD}_{sd}\left(1 - J^{FD}_{d}\right)\right)^K, \end{aligned} \tag{10}$$

where P^{FD}_{sd} is the probability for an arbitrary relay to successfully detect and decode x_2; J^{FD}_{d} represents the probability for the BS to correctly decode x_2 forwarded by an arbitrary relay; and $C^j_K = \frac{K!}{j!(K-j)!}$. P^{FD}_{sd} and J^{FD}_{d} are formulated as

$$\begin{aligned} P^{FD}_{sd} &= \int_0^{\infty} P^{FD}_{d}(x) \Pr\left(\gamma_{D_2 \to D_{1,k}} > T_2\right) f_X(x) dx \\ &= \int_{\frac{\varpi_1\Omega_{LI}\rho + 1}{\rho} T_2}^{\infty} P^{FD}_{d}(x) f_X(x) dx \end{aligned} \tag{11}$$

$$\begin{aligned} J^{FD}_{d} &= \Pr\left(\gamma_{D_2 \to D_{1,k} \to BS, MAX} > T_2\right) \\ &= \Pr\left(|h_{1,k}|^2\rho > T_2\right) \approx e^{-\left(1 + d^{\alpha}_{D_2,BS}\right)\frac{T_2}{\rho}}, \end{aligned} \tag{12}$$

where $P^{FD}_{d}(x)$ is the detection probability of ED by $D_{1,k}$ to detect x_2. It is a function associated with $|h_{2,k}|^2$, which is denoted as x. $f_X(x)$ is the probability density function (PDF) of x. On the condition of $d_{1,k} = \sqrt{d^2_{D_2,BS} + r^2_{2,k} - 2d_{D_2,BS}r_{2,k}\cos(\theta_k)}$ and $d_{1,k} \gg r_{2,k}$ as stated in Section 2.1, the distance between $D_{1,k}$ and the BS is approximated as the distance between the BS and D_2, that is $d_{1,k} \approx d_{D_2,BS}$ [4]. According to the central limit theorem, the

detection probability $P_d^{FD}(x)$ is

$$P_d^{FD}(x) = \mathcal{Q}\left(\frac{\mathcal{Q}^{-1}(P_f^{pre})\sqrt{\frac{2}{L}}(1+\varpi_1\Omega_{LI}\rho)-\rho x}{\sqrt{2/L}(1+\varpi_1\Omega_{LI}\rho+\rho x)}\right), \quad (13)$$

where $\mathcal{Q}(\cdot)$ is the Marcum Q-function. Moreover, relays are uniformly distributed within the disc around D_2. Thus, the PDF of $r_{2,k}$ is $f_R(r_{2,k}) = \frac{2r_{2,k}}{R_D^2}$. Given $h_{2,k} = \frac{h'}{\sqrt{1+r_{2,k}^{\alpha}}}$, the cumulative distribution function (CDF) of $|h_{2,k}|^2$ is expressed as

$$F_X(x) = \int_0^{R_D}\left(1-e^{-\left(1+r_{2,k}^{\alpha}\right)x}\right)\frac{2r_{2,k}}{R_D^2}dr_{2,k}. \quad (14)$$

According to Gaussian-Chebyshev quadrature [32], $F_X(x)$ is further calculated as $F_X(x) \approx \frac{\pi}{2N}\sum_{n=1}^{N}\sqrt{1-\phi_n^2}(1-e^{-c_n x})(\phi_n+1)$, where $c_n = 1+(\frac{R_D}{2}(\phi_n+1))^{\alpha}$ and $\phi_n = \cos(\frac{2n-1}{2N}\pi)$ [4]. N is the complexity-vs-accuracy tradeoff parameter. Therefore, the PDF of $|h_{2,k}|^2$ is

$$f_X(x) \approx \frac{\pi}{2N}\sum_{n=1}^{N}\sqrt{1-\phi_n^2}(\phi_n+1)c_n e^{-c_n x}. \quad (15)$$

Substituting (13) and (15) into (11), the expression of P_{sd}^{FD} can be obtained as shown in (16) and (17) after tedious algebraic manipulations and integral calculations.

$$P_{sd}^{FD} = \frac{\pi}{4N}\sum_{n=1}^{N}\left(\sqrt{1-\phi_n^2}(\phi_n+1)e^{-p_n T_2}\right) - \frac{\sqrt{\pi}}{2N}\frac{p_n}{c_n}$$
$$\times\sum_{\psi=0}^{\infty}\sum_{n=1}^{N}\frac{(-1)^{\psi}\left(\frac{1}{\sqrt{2}}\right)^{2\psi+1}}{(\psi!)(2\psi+1)}\sqrt{1-\phi_n^2}(\phi_n+1)c_n e^{p_n}\Theta_{n,\psi} \quad (16)$$

$$\Theta_{n,\psi} = \left(-\sqrt{\frac{L}{2}}\right)^{2\psi+1}\frac{e^{-p_n(T_2+1)}}{p_n} + \sum_{\xi=1}^{2\psi+1}C_{2\psi+1}^{\xi}\left(-\sqrt{\frac{L}{2}}\right)^{2\psi+1-\xi}$$
$$\times B^{\xi}\left(\frac{(-1)^{\xi}p_n^{\xi-1}\mathrm{Ei}(-p_n u)}{(\xi-1)!} + \frac{e^{-p_n u}}{u^{\xi-1}}\sum_{\omega=0}^{\xi-2}\frac{(-1)^{\omega}p_n^{\omega}u^{\omega}}{(\xi-1)(\xi-2)\cdots(\xi-\omega-1)}\right), \quad (17)$$

where $B = \frac{\mathcal{Q}^{-1}(P_f^{pre})\sqrt{2/L}+1}{\sqrt{2/L}}$, $u = T_2+1$, $p_n = c_n\frac{\varpi_1\Omega_{LI}\rho+1}{\rho}$ and $\mathrm{Ei}(\cdot)$ is the exponential integral function.

Substituting J_d^{FD} and P_{sd}^{FD} obtained from (12), (16) and (17) into (10), we get the outage probability $P_{D_2}^{TRSPA-FD}$.

Corollary 1. *On the basis of the derivation result (10) for TRSPA-FD, we make the following changes to obtain the outage probabilities $P_{D_2}^{TRSPA-HD}$ and $P_{D_2}^{TRSPA-OMA}$ of D_2 for TRSPA-HD and TRSPA-OMA, which respectively refer to TRSPA working in HD-CNOMA and COMA schemes: (i) substitute $\varpi_1 = 0$ into (10) since HD-CNOMA and COMA are not affected by LI and (ii) change T_2 into $\phi_{HD,2} = 2^{2R_2}-1$ and $\phi_{OMA,2} = 2^{3R_2}-1$ which are the target SNRs during decoding x_2 in HD-CNOMA and COMA schemes, respectively, since each of their entire transmission processes finish in two or three time slots based on Section 2.3.*

We further analyze the diversity order for D_2 which is defined as

$$d_{D_2}^{TRSPA-FD} = -\lim_{\rho\to\infty}\frac{\lg\left(P_{D_2}^{TRSPA-FD}\right)}{\lg\rho}. \quad (18)$$

When $\rho\to\infty$, we get $\lim_{\rho\to\infty}J_d^{FD} \triangleq J_d^{FD,\infty} \approx 1$ based on (12) and $e^{-\frac{1}{\rho}} \approx 1-\frac{1}{\rho}$. With $\lim_{\rho\to\infty}\frac{\varpi_1\Omega_{LI}\rho+1}{\rho} = \varpi_1\Omega_{LI}$, we obtain the asymptotic value of P_{sd}^{FD}, that is $\lim_{\rho\to\infty}P_{sd}^{FD} = P_{sd}^{FD,\infty} \triangleq P_{SD}^{FD}$. Given (10), the asymptotic outage probability of D_2 for TRSPA-FD is

$$\lim_{\rho\to\infty}P_{D_2}^{TRSPA-FD} \triangleq P_{D_2}^{TRSPA-FD,\infty} = \left(1-P_{SD}^{FD}\right)^K. \quad (19)$$

Substituting (19) into (18), we learn that D_2's diversity order equals zero, that is $d_{D_2}^{TRSPA-FD} = 0$.

Remark 1. The diversity order of TRSPA-FD is zero due to the effect of residual LI. Therefore, a floor exists for D_2's outage probability.

As to TRSPA-HD, according to (11), its successful detecting and decoding probability P_{sd}^{HD} when $\rho\to\infty$ is approximated as $P_{sd}^{HD,\infty} = \lim_{\rho\to\infty}\int_{\frac{\phi_{HD,2}}{\rho}}^{\infty}P_d^{HD}(x)f_X(x)dx$, where $P_d^{HD}(x)$ is the detection probability of an arbitrary relay in a TRSPA-HD system. $\lim_{\rho\to\infty}P_d^{HD}(x) = \mathcal{Q}\left(\frac{\mathcal{Q}^{-1}(P_f^{pre})\sqrt{2/L}-\rho x}{\sqrt{2/L}(1+\rho x)}\right)$ according to (13). Therefore, $P_{sd}^{HD,\infty}$ is further written as $P_{sd}^{HD,\infty} = \lim_{\rho\to\infty}\int_{\frac{\phi_{HD,2}}{\rho}}^{\infty}f_X(x)dx = 1-\lim_{\rho\to\infty}F_X(\frac{\phi_{HD,2}}{\rho})$. According to (14), $\lim_{\rho\to\infty}F_X(\frac{\phi_{HD,2}}{\rho})$ is approximated as $\lim_{\rho\to\infty}\frac{\phi_{HD,2}}{\rho}\int_0^{R_D}(1+r_{2,k}^{\alpha})\frac{2r_{2,k}}{R_D^2}dr_{2,k}$. Let $R = \int_0^{R_D}(1+r_{2,k}^{\alpha})\frac{2r_{2,k}}{R_D^2}dr_{2,k} = 1+\frac{2}{\alpha+2}R_D^{\alpha}$ and we get $\lim_{\rho\to\infty}F_X(\frac{\phi_{HD,2}}{\rho}) \approx \lim_{\rho\to\infty}R\frac{\phi_{HD,2}}{\rho}$. Then $P_{sd}^{HD,\infty} = 1-\lim_{\rho\to\infty}F_X(\frac{\phi_{HD,2}}{\rho}) \approx 1-\lim_{\rho\to\infty}R\frac{\phi_{HD,2}}{\rho}$. Based on (10), the

asymptotic outage probability of D_2 for TRSPA-HD when $\rho \to \infty$ is

$$P_{D_2}^{TRSPA-HD,\infty} = \left(\left(1 + d_{D_2,BS}^{\alpha}\right)\phi_{HD,2} + R\phi_{HD,2}\right)^K \left(\frac{1}{\rho}\right)^K. \tag{20}$$

Substituting (20) into (18), we get $d_{D_2}^{TRSPA-HD} = K$.

Similarly, we also work out the asymptotic outage probability of D_2 for TRSPA-OMA:

$$P_{D_2}^{TRSPA-OMA,\infty} = \left(\left(1 + d_{D_2,BS}^{\alpha}\right)\phi_{OMA,2} + R\phi_{OMA,2}\right)^K \left(\frac{1}{\rho}\right)^K. \tag{21}$$

Substituting (21) into (18), we learn that the diversity order for TRSPA-OMA equals K.

Remark 2. Diversity orders of TRSPA for HD-CNOMA and COMA schemes both equal K.

3.1.2 | Outage probability of D_2 and diversity analysis under H_0

D_2 does not exist herein.

3.2 | Ergodic rate of D_{1,k^*}

3.2.1 | Ergodic rate of D_{1,k^*} and spatial multiplexing gain under H_1

The CDF $F_Y(y)$ of the received SNR (i.e. Y) at the BS when decoding x_{1,k^*} is a critical parameter when deriving D_{1,k^*}'s ergodic rate. We next work out $F_Y(y)$ in three independent cases.

The first case $E_{1,j}$ refers to $|\mathcal{S}_1| = j \neq 0$ and $|\mathcal{S}_2| = 0$, which means none of the j relays within $\mathcal{S}_1$ could enable the BS to successfully decode x_2 even if they allocate all power to x_2. $k^* = \arg\max_k \{|h_{1,k}|^2 : D_{1,k} \in \mathcal{S}\}$ according to Section 2.3. Then the received SINR at the BS to decode x_{1,k^*} is $\hat{\gamma}_{D_{1,k^*}\to BS}|E_{1,j} = \max_{k\in\mathcal{S}} |h_{1,k}|^2\rho \triangleq Y|E_{1,j}$. In the second case $E_{2,i,j}$ when $|\mathcal{S}_1| = j \neq 0$ and $|\mathcal{S}_2| = i \neq 0$, $k^* = \arg\max_k \{|h_{1,k}|^2 : D_{1,k} \in \mathcal{S}_2\}$ according to (7) and $a_{1,k^*} = \frac{|h_{1,k^*}|^2\rho - T_2}{|h_{1,k^*}|^2\rho(1+T_2)}$ according to (8). Then the received SINR value under $E_{2,i,j}$ at the BS to decode x_{1,k^*} is $\gamma_{D_{1,k^*}\to BS}|E_{2,i,j} = \max_{k\in\mathcal{S}_2} a_{1,k}|h_{1,k}|^2\rho = \max_{k\in\mathcal{S}_2} \frac{|h_{1,k}|^2\rho - T_2}{1+T_2} \triangleq Y|E_{2,i,j}$. As to the third case E_3 when $|\mathcal{S}_1| = 0$, similar with $E_{1,j}$, $k^* = \arg\max_k \{|h_{1,k}|^2 : D_{1,k} \in \mathcal{S}\}$ according to Section 2.3. Then the received SINR under E_3 at the BS to decode x_{1,k^*} is $\hat{\gamma}_{D_{1,k^*}\to BS}|E_3 = \max_{k\in\mathcal{S}} |h_{1,k}|^2\rho \triangleq Y|E_3$.

Given the fact that the outage probability of a practical system is usually extremely small to guarantee the reliability and robustness [3, 33], the CDF of Y can be formulated as (22) by combining all these three cases.

$$\begin{aligned}
F_Y(y) &= \sum_{j=1}^{K} \Pr(|\mathcal{S}_1| = j \neq 0,\ |\mathcal{S}_2| = 0) \\
&\quad \Pr\left(\left(\hat{\gamma}_{D_{1,k^*}\to BS}\middle|E_{1,j}\right) < y\right) + \Pr(|\mathcal{S}_1| = 0) \\
&\quad \Pr\left(\left(\hat{\gamma}_{D_{1,k^*}\to BS}\middle|E_3\right) < y\right) \\
&\quad + \sum_{j=1}^{K}\sum_{i=1}^{j} \Pr(|\mathcal{S}_1| = j \neq 0,\ |\mathcal{S}_2| = i \neq 0) \\
&\quad \Pr\left(\left(\gamma_{D_{1,k^*}\to BS}\middle|E_{2,i,j}\right) < y\right) \\
&= \sum_{j=1}^{K} C_K^j \left(P_{sd}^{FD}\right)^j \left(1 - P_{sd}^{FD}\right)^{K-j} \left(1 - J_d^{FD}\right)^j \left(1 - e^{-\left(1+d_{D_2,BS}^{\alpha}\right)\frac{y}{\rho}}\right)^K \\
&\quad + \left(1 - P_{sd}^{FD}\right)^K \left(1 - e^{-\left(1+d_{D_2,BS}^{\alpha}\right)\frac{y}{\rho}}\right)^K \\
&\quad + \sum_{j=1}^{K} C_K^j \left(P_{sd}^{FD}\right)^j \left(1 - P_{sd}^{FD}\right)^{K-j} \\
&\left(\sum_{i=1}^{j} C_j^i \left(J_d^{FD}\right)^i \left(1 - J_d^{FD}\right)^{j-i} \left(1 - e^{-\left(1+d_{D_2,BS}^{\alpha}\right)\frac{(1+T_2)y + T_2}{\rho}}\right)^i\right).
\end{aligned} \tag{22}$$

The achievable rate of D_{1,k^*} is $R_{D_{1,k^*}}^{TRSPA-FD}|H_1 = \log(1+Y)$. Then the ergodic rate under H_1 is $E[R_{D_1}^{TRSPA-FD}|H_1] = E[\log(1+Y)] = \frac{1}{\ln 2}\int_0^\infty \frac{1}{1+y}(1 - F_Y(y))dy$ [17, 21]. According to $\int_0^\infty \frac{1}{1+y} e^{-(1+d_{D_2,BS}^{\alpha})\frac{y}{\rho}m} dy = -e^{(1+d_{D_2,BS}^{\alpha})\frac{m}{\rho}} \mathrm{Ei}(-(1+d_{D_2,BS}^{\alpha})\frac{m}{\rho})$ [34] and (22), we have

$$E\left[R_{D_{1,k^*}}^{TRSPA-FD}|H_1\right] = J_1 + J_2 + J_3, \tag{23}$$

where

$$\begin{aligned}
J_1 &= \frac{1}{\ln 2}\sum_{j=1}^{K} C_K^j \left(P_{sd}^{FD}\right)^j \left(1 - P_{sd}^{FD}\right)^{K-j} \left(1 - J_d^{FD}\right)^j \\
&\times \left(\sum_{m=1}^{K} C_K^m (-1)^m e^{\left(1+d_{D_2,BS}^{\alpha}\right)\frac{m}{\rho}} \mathrm{Ei}\left(-\frac{\left(1 + d_{D_2,BS}^{\alpha}\right)m}{\rho}\right)\right),
\end{aligned} \tag{24}$$

$$J_2 = \frac{1}{\ln 2}\sum_{j=1}^{K} C_K^j \left(P_{sd}^{FD}\right)^j \left(1-P_{sd}^{FD}\right)^{K-j} \sum_{i=1}^{j} C_j^i \left(J_d^{FD}\right)^i \times \left(1-J_d^{FD}\right)^{j-i} \sum_{m=1}^{i} C_i^m (-1)^m e^{\frac{\left(1+d_{D_2,BS}^{\alpha}\right)(1+2T_2)m}{\rho}} \times \mathrm{Ei}\left(-\frac{\left(1+d_{D_2,BS}^{\alpha}\right)(1+T_2)m}{\rho}\right), \tag{25}$$

$$J_3 = \frac{1}{\ln 2}\left(1-P_{sd}^{FD}\right)^K \times \sum_{m=1}^{K} C_K^m (-1)^m e^{\left(1+d_{D_2,BS}^{\alpha}\right)\frac{m}{\rho}} \mathrm{Ei}\left(-\frac{\left(1+d_{D_2,BS}^{\alpha}\right)m}{\rho}\right). \tag{26}$$

Corollary 2. *Based on (23) for TRSPA-FD, we make the following changes to obtain the ergodic rate of TRSPA-HD: (i) let* $\varpi_1 = 0$*; (ii) change* T_2 *into* $\phi_{HD,2} = 2^{2R_2} - 1$*; and (iii) rewrite (23) into* $E[R_{D_{1,k^*}}^{TRSPA-HD}|H_1] = \frac{1}{2}(J_1 + J_2 + J_3)$*. As to TRSPA-OMA, besides assigning* $\varpi_1 = 0$*, changing* T_2 *into* $\phi_{OMA,2} = 2^{3R_2} - 1$*, and rewriting (23) into* $E[R_{D_{1,k^*}}^{TRSPA-OMA}|H_1] = \frac{2}{3}J_1 + \frac{1}{3}J_2 + \frac{2}{3}J_3$*, J_2 also needs to be modified into $J_{OMA,2}$ as (27),*

$$J_{OMA,2} = \frac{1}{\ln 2}\sum_{j=1}^{K} C_K^j \left(P_{sd}^{OMA}\right)^j \left(1-P_{sd}^{OMA}\right)^{K-j} \times \sum_{i=1}^{j} C_j^i \left(J_d^{OMA}\right)^i \left(1-J_d^{OMA}\right)^{j-i} \sum_{m=1}^{i} C_i^m (-1)^m e^{\left(1+d_{D_2,BS}^{\alpha}\right)\frac{m}{\rho}} \mathrm{Ei}\left(-\frac{\left(1+d_{D_2,BS}^{\alpha}\right)m}{\rho}\right) \tag{27}$$

where the parameters P_{sd}^{OMA} and J_d^{OMA} are defined in a TRSPA-OMA scheme with the same physical meanings as P_{sd}^{FD} and J_d^{FD} in (11) and (12).

Then we evaluate the slope of the ergodic rate curve in the high SNR region. Its physical meaning is spatial multiplexing gain [35]. It is defined as

$$S_{D_{1,k^*}}^{TRSPA-FD}|H_1 = \lim_{\rho\to\infty} \frac{E\left[R_{D_{1,k^*}}^{TRSPA-FD}\middle|H_1\right]}{\log\rho}. \tag{28}$$

Using $\mathrm{Ei}(-\frac{1}{\rho}) \to \ln\frac{1}{\rho} + C_E$ where C_E is the Euler constant, the asymptotic ergodic rate of D_{1,k^*} for TRSPA-FD when $\rho \to \infty$ can be written as (29)-(32) according to (23)-(26).

$$E\left[R_{D_{1,k^*}}^{TRSPA-FD,\infty}|H_1\right] = J_1^{\infty} + J_2^{\infty} + J_3^{\infty}, \tag{29}$$

where J_1, J_2 and J_3 are approximated as $J_1^{\infty}, J_2^{\infty}$ and J_3^{∞} when $\rho \to \infty$, respectively.

$$J_1^{\infty} = 0. \tag{30}$$

$$J_2^{\infty} = \frac{1}{\ln 2}\sum_{j=1}^{K} C_K^j \left(P_{SD}^{FD}\right)^j \left(1-P_{SD}^{FD}\right)^{K-j} \sum_{i=1}^{j} C_j^i \times \left(\left(1+d_{D_2,BS}^{\alpha}\right)\frac{T_2}{\rho}\right)^{j-i} \sum_{m=1}^{i} C_i^m (-1)^m \times \left(\ln\frac{\left(1+d_{D_2,BS}^{\alpha}\right)(1+T_2)m}{\rho} + C_E\right). \tag{31}$$

$$J_3^{\infty} = \frac{1}{\ln 2}\left(1-P_{SD}^{FD}\right)^K \times \sum_{m=1}^{K} C_K^m (-1)^m \left(\ln\frac{\left(1+d_{D_2,BS}^{\alpha}\right)m}{\rho} + C_E\right). \tag{32}$$

Accordingly, substituting (30), $\lim_{\rho\to\infty}\frac{J_2^{\infty}}{\log\rho} = \sum_{j=1}^{K} C_K^j (P_{SD}^{FD})^j (1-P_{SD}^{FD})^{K-j} (\sum_{m=1}^{j} C_i^m (-1)^{m+1})$ and $\lim_{\rho\to\infty}\frac{J_3^{\infty}}{\log\rho} = (1-P_{SD}^{FD})^K \sum_{m=1}^{K} C_K^m (-1)^{m+1}$ into (29), we work out the spatial multiplexing gain in (33) for TRSPA-FD.

$$S_{D_{1,k^*}}^{TRSPA-FD}|H_1 = \sum_{j=1}^{K} C_K^j \left(P_{SD}^{FD}\right)^j \left(1-P_{SD}^{FD}\right)^{L-j} \times \sum_{m=1}^{j} C_i^m (-1)^{m+1} + \left(1-P_{SD}^{FD}\right)^K \sum_{m=1}^{K} C_K^m (-1)^{m+1} = 1. \tag{33}$$

Similarly, we also obtain the spatial multiplexing gains $S_{D_{1,k^*}}^{TRSPA-HD}|H_1 = \frac{1}{2}$ and $S_{D_{1,k^*}}^{TRSPA-OMA}|H_1 = \frac{1}{3}$.

In a system with A_1 transmit antennas and A_2 receive antennas, the maximum spatial multiplexing gain is $\min(A_1, A_2)$ [36]. Given the investigated system model in Section 2.1, the maximum spatial multiplexing gain of D_{1,k^*} is 1.

Remark 3. The spatial multiplexing gain for D_{1,k^*} in a TRSPA-FD system under H_1 is 1 and it is the achievable maximum value in the considered system. As to TRSPA-HD and TRSPA-OMA, their spatial multiplexing gains are only $\frac{1}{2}$ and $\frac{1}{3}$.

3.2.2 | Ergodic rate of D_{1,k^*} and spatial multiplexing gain under H_0

Under H_0, all relays cannot obtain D_2's message since D_2 does not exist. According to (9), $k^* = \arg\max_k\{|h_{1,k}|^2 : D_{1,k} \in \mathcal{S}\}$. Then D_{1,k^*}'s data rate is $R^{TRSPA-FD}_{D_{1,k^*}}|H_0 = \log(1+\hat{\gamma}_{D_{1,k^*}\to BS}) = \log(1+|h_{1,k^*}|^2\rho)$. Therefore, the ergodic rate of D_{1,k^*} is $E[R^{TRSPA-FD}_{D_{1,k^*}}|H_0] = E[\log(1+\underbrace{\max|h_{1,k}|^2\rho}_{\hat{Y}})] = \frac{1}{\ln 2}\int_0^\infty \frac{1}{1+\hat{y}}(1-F_{\hat{Y}}(\hat{y}))d\hat{y}$, where $F_{\hat{Y}}(\hat{y})$ is the CDF of $\hat{Y}$. We know that $F_{\hat{Y}}(\hat{y}) = \Pr(\max|h_{1,k}|^2\rho < \hat{y}) = (1-e^{-(1+d^\alpha_{D_2,BS})\frac{\hat{y}}{\rho}})^K$. The ergodic rate of D_{1,k^*} under H_0 is thus written as $E[R^{TRSPA-FD}_{D_{1,k^*}}|H_0] = \frac{1}{\ln 2}\int_0^\infty \frac{1}{1+\hat{y}}(\sum_{j=1}^K C_K^j(-1)^j e^{-(1+d^\alpha_{D_2,BS})\frac{\hat{y}}{\rho}j})d\hat{y}$. According to [34], we further get

$$E\left[R^{TRSPA-FD}_{D_{1,k^*}}|H_0\right] = \frac{1}{\ln 2}\sum_{j=1}^K C_K^j(-1)^j \times\left(-e^{\left(1+d^\alpha_{D_2,BS}\right)\frac{j}{\rho}}\mathrm{Ei}\left(-\left(1+d^\alpha_{D_2,BS}\right)\frac{j}{\rho}\right)\right). \tag{34}$$

Corollary 3. *Ergodic rates of D_{1,k^*} under H_0 for TRSPA-HD and TRSPA-OMA are written as*

$$E\left[R^{TRSPA-HD}_{D_{1,k^*}}|H_0\right] = \frac{1}{2\ln 2}\sum_{j=1}^K C_K^j(-1)^j \times\left(-e^{\left(1+d^\alpha_{D_2,BS}\right)\frac{j}{\rho}}\mathrm{Ei}\left(-\left(1+d^\alpha_{D_2,BS}\right)\frac{j}{\rho}\right)\right) \tag{35}$$

$$E\left[R^{TRSPA-OMA}_{D_{1,k^*}}|H_0\right] = \frac{2}{3\ln 2}\sum_{j=1}^K C_K^j(-1)^j \times\left(-e^{\left(1+d^\alpha_{D_2,BS}\right)\frac{j}{\rho}}\mathrm{Ei}\left(-\left(1+d^\alpha_{D_2,BS}\right)\frac{j}{\rho}\right)\right). \tag{36}$$

We know that $\mathrm{Ei}(-\frac{1}{\rho}) \approx \ln\frac{1}{\rho} + C_E$ and $e^{-\frac{1}{\rho}} \approx 1-\frac{1}{\rho}$ when $\rho\to\infty$. Based on (34), the asymptotic ergodic rate of D_{1,k^*} under H_0 for TRSPA-FD is written as

$$E\left[R^{TRSPA-FD,\infty}_{D_{1,k^*}}|H_0\right] = \frac{-1}{\ln 2}\sum_{j=1}^K C_K^j(-1)^j\left(\ln\frac{\left(1+d^\alpha_{D_2,BS}\right)j}{\rho} + C_E\right). \tag{37}$$

Substituting (37) into (28), the spatial multiplexing gain of TRSPA-FD is worked out to be 1, that is $S^{TRSPA-FD}_{D_{1,k^*}}|H_0 = 1$. Similarly, spatial multiplexing gains of TRSPA-HD and TRSPA-OMA are $\frac{1}{2}$ and $\frac{2}{3}$, that is $S^{TRSPA-HD}_{D_{1,k^*}}|H_0 = \frac{1}{2}$ and $S^{TRSPA-OMA}_{D_{1,k^*}}|H_0 = \frac{2}{3}$.

Remark 4. The spatial multiplexing gain for D_{1,k^*} in a TRSPA-FD system under H_0 is 1 and it is the achievable maximum value of our considered system. As to TRSPA-HD and TRSPA-OMA, their spatial multiplexing gains are only $\frac{1}{2}$ and $\frac{2}{3}$.

4 | PERFORMANCE COMPARISON

The above section already considers the impact of residual LI caused by the practical assumption of imperfect self-interference cancellation. According to Remarks 1–4 and research findings associated with CNOMA, FD-CNOMA outperforms HD-CNOMA and COMA in the low SNR region. However, it gradually loses its advantage as SNR increases, since LI gets stronger in the high SNR region. The intensity of LI seems to be the dominant factor of performance comparison result. Motivated by this, we further presents comparison results under the consideration of reasonable LI intensity to explicitly answer the question which relaying mode the proposed TRSPA strategy should choose in practice.

4.1 | Outage probability

The general comparison result of FD-relaying-related research works [17–19] is that FD performs better than HD and OMA in the low SNR region but it will be outperformed in the high SNR region. It is of great practical significance to compare the results of TRSPA-FD, TRSPA-HD and TRSPA-OMA with reasonable SI suppression capabilities, especially in the high SNR region.

Based on [10] and [29], existing SI suppression techniques are able to reduce the intensity of LI to the same level as noise floor, that is $\Omega_{LI}P_r = N_0$. Substituting $\Omega_{LI}P_r = N_0$ into (11) and (13), when $\rho\to\infty$, P^{FD}_{sd} of TRSPA-FD is approximated as

$$P^{FD,\infty}_{sd,\,LI=noi} = \lim_{\rho\to\infty}\int_{\frac{2T_2}{\rho}}^\infty P^{FD}_d(x)f_X(x)dx \approx 1-\lim_{\rho\to\infty}F_X\left(\frac{2T_2}{\rho}\right) = 1-\lim_{\rho\to\infty}R\frac{2T_2}{\rho}. \tag{38}$$

The asymptotic outage probability of TRSPA-FD in (19) becomes

$$P^{TRSPA-FD,\infty}_{D_2,\,LI=noi} = \left(\left(1+d^\alpha_{D_2,BS}\right)T_2 + 2RT_2\right)^K\left(\frac{1}{\rho}\right)^K. \tag{39}$$

Substituting (39) into (18), the corresponding diversity order is worked out as $d_{D_2,\,LI=noi}^{TRSPA-FD} = -\lim_{\rho\to\infty}\frac{\lg(P_{D_2,\,LI=noi}^{TRSPA-FD,\infty})}{\lg\rho} = K$ in a practical scenario. The outage probability of TRSPA-FD therefore decreases at the same rate as TRSPA-HD and TRSPA-OMA as ρ gets larger. Also, their performance comparison result will not fluctuate with the change of ρ. The one with a better performance is always better. We next need to further demonstrate that FD is the best one.

We define the outage performance gain of TRSPA-FD over TRSPA-HD as $G_{FD,\,HD} = -10\lg\frac{P_{D_2,\,LI=noi}^{TRSPA-FD,\infty}}{P_{D_2}^{TRSPA-HD,\infty}}$. According to (39) and (20), $G_{FD,\,HD}$ is calculated as

$$G_{FD,\,HD} = -10K\lg\frac{\left(\left(1+d_{D_2,BS}^{\alpha}\right)T_2+2RT_2\right)}{\left(\left(1+d_{D_2,BS}^{\alpha}\right)\phi_{HD,2}+R\phi_{HD,2}\right)}. \tag{40}$$

Since $\phi_{HD,2} - T_2 = (2^{R_2}-1)^2 > 0$ is true for any positive number R_2, we have $\phi_{HD,2} > 2T_2 > T_2$. Thus, $G_{FD,\,HD}$ is positive, verifying that TRSPA-FD achieves a better outage performance than TRSPA-HD. The outage performance gain of TRSPA-FD compared to TRSPA-OMA is

$$G_{FD,\,OMA} = -10K\lg\frac{\left(\left(1+d_{D_2,BS}^{\alpha}\right)T_2+2RT_2\right)}{\left(\left(1+d_{D_2,BS}^{\alpha}\right)\phi_{OMA,2}+R\phi_{OMA,2}\right)}. \tag{41}$$

Since $\phi_{OMA,2} > \phi_{HD,2} > 2T_2 > T_2$, $G_{FD,\,OMA}$ must be a positive constant.

Remark 5. Given reasonable SI suppression capabilities, TRSPA-FD always achieves better outage performance than TRSPA-HD and TRSPA-OMA and it will never be exceeded no matter how large the SNR is. Therefore, different from the general conclusion of other researchers, we confirm that FD is the outage-optimal choice when designing a practical TRSPA system.

4.2 | Ergodic rate

We substitute $\Omega_{LI}P_r = N_0$ into (30), (31) and (32). By using (38), they become $J_{1,\,LI=noi}^{\infty} = 0$, $J_{2,\,LI=noi}^{\infty} = \frac{1}{\ln 2}\sum_{j=1}^{K}C_K^j(P_{sd,\,LI=noi}^{FD})^j \times(1-P_{sd,\,LI=noi}^{FD})^{K-j}\sum_{i=1}^{j}C_j^i(\frac{(1+d_{D_2,BS}^{\alpha})T_2}{\rho})^{j-i}\times\sum_{m=1}^{i}C_i^m(-1)^m\ln(\frac{(1+d_{D_2,BS}^{\alpha})(1+T_2)m}{\rho}+C_E)$ and $J_{3,\,LI=noi}^{\infty} = 0$. Furthermore, we have $\lim_{\rho\to\infty}\frac{J_{1,\,LI=noi}^{\infty}+J_{2,\,LI=noi}^{\infty}+J_{3,\,LI=noi}^{\infty}}{\log\rho} = \lim_{\rho\to\infty}\sum_{i=1}^{K}C_K^i((1+d_{D_2,BS}^{\alpha})\frac{T_2}{\rho})^{K-i} = 1$. According to (28) and (29), the spatial multiplexing gain of D_{1,k^*} for TRSPA-FD in practical scenarios is equal to 1, which is the same as Remark 3.

Remark 6. Given reasonable SI suppression capabilities of FD user relays, the spatial multiplexing gain of TRSPA-FD still achieves 1, which is the same as Remark 3. It is the maximum achievable value, and is larger than those of TRSPA-HD and TRSPA-OMA.

However, there is only one concern about the superiority illustration of TRSPA-FD in terms of ergodic rate. According to Section 4, TRSPA-HD and TRSPA-OMA always achieve worse outage performance than TRSPA-FD. Their user relays are more likely to fail to obtain x_2. So they tend to allocate more power to relays in order to fully utilize the power resources according to the proposed TRSPA stated in Section 2.3. In such cases, these benchmarks may achieve larger ergodic rates than TRSPA-FD, however, at the cost of worse outage performance. As stated in Section 1, the transmissions of user relays' messages are executed on the condition that D_2's QoS requirement is satisfied. Such a sacrifice of outage performance is not allowed. Moreover, the ergodic rate comparison under unequal premises of outage probabilities is not fair. Motivated by these, we next compare TRSPA-FD's ergodic rate with the benchmarks under the same constraint of predetermined outage performance requirement.

Given the preset outage performance requirement P_{out}^{req}, the outage probability obtained from (21) is directly set to be P_{out}^{req}. Then the required transmit SNR by TRSPA-OMA is

$$\rho_{req} = (1+d_{D2,BS}^{\alpha}+R)(2^{3R_2}-1)/(P_{out}^{req})^{\frac{1}{K}}. \tag{42}$$

According to $E[R_{D_{1,k^*}}^{TRSPA-OMA,\infty}|H_1] = \frac{1}{3\ln 2}\sum_{m=1}^{K}C_K^m(-1)^{m+1}(\ln\frac{(1+d_{SB}^{\alpha})m}{\rho_{req}}+C_E)$, the derivative function $\frac{d(E[R_{D_{1,k^*}}^{TRSPA-OMA,\infty}|H_1])}{d(\log\rho_{req})} = \frac{1}{3}$ is obtained. We know from (42) that ρ_{req} is determined by R_2 and it increases with R_2. Thus, we need to further work out the derivative function with respect to the independent variable R_2. Let $W = (1+d_{D_2,BS}^{\alpha}+R)/(P_{out}^{req})^{\frac{1}{K}}$. Then ρ_{req} can be written as $W(2^{3R_2}-1)$ based on (42). Accordingly, the derivative of $\log\rho_{req}$ with respect to R_2 is approximated as $\frac{d(\log\rho_{req})}{d(R_2)}\approx 3$. Therefore, under the restriction of P_{out}^{req}, $E[R_{D_{1,k^*}}^{TRSPA-OMA,\infty}|H_1]$ rises at a rate of $\frac{d(E[R_{D_{1,k^*}}^{TRSPA-OMA,\infty}|H_1])}{d(R_2)}\approx\frac{1}{3}\times 3 = 1$ regarding R_2.

As to TRSPA-FD, its SNR is ρ_{req} as well for comparison fairness. We substitute $\Omega_{LI}P_r = N_0$ and $T_2 = (\frac{\rho_{req}}{W}+1)^{\frac{1}{3}}-1$ into (30), (31) and (32). Then by using (38), they become $J_{1,\,LI=noi}^{\infty} = 0$, $J_{2,\,LI=noi}^{\infty} = \frac{1}{\ln 2}\sum_{m=1}^{K}C_K^m(-1)^m(\ln\frac{(1+d_{D_2,BS}^{\alpha})(\frac{\rho_{req}}{W}+1)^{\frac{1}{3}}m}{\rho_{req}}+C_E)$ and $J_{3,\,LI=noi}^{\infty} = 0$, respectively. Therefore, we get $\lim_{\rho\to\infty}\frac{J_{1,\,LI=noi}^{\infty}+J_{2,\,LI=noi}^{\infty}+J_{3,\,LI=noi}^{\infty}}{\log\rho} = \frac{2}{3}$. According to (29),

we learn that $\lim_{\rho\to\infty}\frac{E[R_{D_{1,k^*}}^{TRSPA-FD,\infty}|H_1]}{\log\rho}=\frac{2}{3}$ in this case. $E[R_{D_{1,k^*}}^{TRSPA-FD,\infty}|H_1]$ increases at a rate of $\frac{d(E[R_{D_{1,k^*}}^{TRSPA-FD,\infty}|H_1])}{d(R_2)}=\frac{d(E[R_{D_{1,k^*}}^{TRSPA-FD,\infty}|H_1])}{d(\log\rho_{req})}\frac{d(\log\rho_{req})}{d(R_2)}\approx\frac{2}{3}\times 3=2$. Similarly, as R_2 rises, the ergodic rate for TRSPA-HD rises at a rate of $\frac{d(E[R_{D_{1,k^*}}^{TRSPA-HD,\infty}|H_1])}{d(R_2)}\approx\frac{1}{6}\times 3=\frac{1}{2}$.

Noted that TRSPA-OMA's outage probability is set to be P_{out}^{req} as shown in (42). We learn from (40) and (41) that the outage probabilities for TRSPA-FD and TRSPA-HD are actually smaller than that of TRSPA-OMA, that is P_{out}^{req}, when they consume the same transmit power ρ_{req}. That is to say, all of these three schemes satisfy the predetermined outage performance requirement. So we summarize Remark 7.

Remark 7. Under the same restriction of the preset outage performance requirement, as R_2 increases (i.e. the required SNR ρ_{req} gets larger correspondingly), the ergodic rates of TRSPA-FD, TRSPA-HD and TRSPA-OMA increase at rates of 2, $\frac{1}{2}$ and 1, respectively.

In conclusion, on the premise that the outage performance requirement is guaranteed, TRSPA-FD's ergodic rate rises the most rapidly in the high SNR region. Together with its superior performance presented in subsequent simulation comparison where SNR rises from a small value, we confirm that FD is always the ergodic-rate-optimal choice for a TRSPA system, regardless of the value of SNR.

5 | NUMERICAL RESULTS

We present numerical simulation results to (i) validate the derived expressions in Section 3; (ii) compare the performance of our proposed TRSPA with various benchmarks introduced in Section 2.3, including Max-Min [30], SRS [4] and TRS [11], and (iii) verify the superiority of TRSPA-FD over TRSPA-HD and TRSPA-OMA, where TRSPA-FD, TRSPA-HD and TRSPA-OMA refer to the proposed TRSPA strategy working in FD-CNOMA [6], HD-CNOMA [31] and COMA [17] schemes, respectively. Unless otherwise stated, the simulation parameters are summarized as follows: $\alpha=2$, $R_D=2$ m, $d_{D_2,BS}=10$ m, $N=15$ and $K=2$ [4], $L=30$ and $P_f^{pre}=0.1$ [6]; power coefficients of relays for benchmarks are $a_{1,k}^{Max-Min}=a_{1,k}^{SRS}=a_{1,k}^{TRS}=0.25$ [11]; $R_2=0.5$ bit per channel user (BPCU) and $\Omega_{LI}=-15$ dB [17].

We compare the simulated outage performance of D_2 versus transmit SNR for the proposed TRSPA-FD scheme with different Ω_{LI}s and other benchmarks under H_1 in Figure 2. Corresponding theoretical derivation results are presented in Figure 3 to validate the correctness. In Figure 3, the exact results of TRSPA-FD, TRSPA-HD and TRSPA-OMA are worked out based on (10) and Corollary 1, respectively. Outage floor of

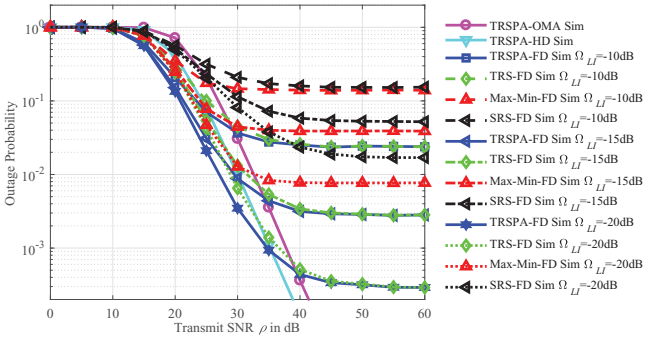

FIGURE 2 Simulated outage probabilities of D_2 versus transmit SNR for TRSPA-FD and benchmarks with different Ω_{LI}s under the hypothesis of H_1

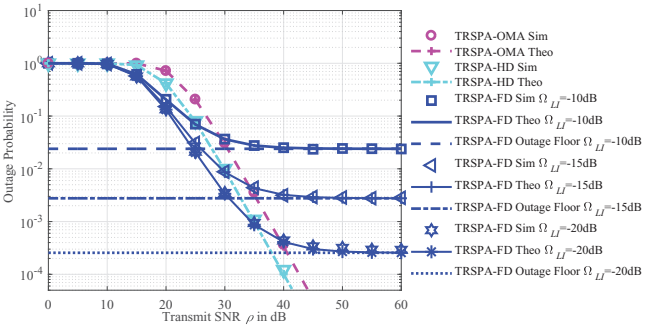

FIGURE 3 Exact and simulated outage probabilities of D_2 versus transmit SNR for TRSPA-FD and benchmarks with different Ω_{LI}s under the hypothesis of H_1

TRSPA-FD is obtained from (19). The well-matched simulation and exact results and the well-approximated simulation results and outage floors validate these derived results. An outage floor for TRSPA-FD exists in Figure 3 due to effects of residual LI in a FD relaying mode, verifying Remark 1. When it comes to the performance comparison, it is observed from Figure 2 that the proposed TRSPA strategy with proper power allocation coefficients always achieves better outage performance than other RS strategies, verifying Theorem 1. As to TRSPA applied to different relaying modes, TRSPA-FD outperforms TRSPA-HD and TRSPA-OMA in the low SNR region, since TRSPA-FD completes each transmission process of D_2 in one time slot while TRSPA-HD and TRSPA-OMA, respectively, need two and three time slots. However, as SNR gets larger, over 30 dB in the case of $\Omega_{LI}=-15$ dB, the outage performance of TRSPA-FD is outperformed by benchmarks, since the intensity of LI gradually becomes stronger, limiting the outage performance of FD mode. This conclusion is consistent with those in [17, 18] and [19]. We also learn from Figure 2 that a smaller LI cancellation coefficient leads to a better outage performance.

According to [10] and [29], existing SI suppression techniques are capable of reducing the intensity of LI to the same level as noise floor, which means $\Omega_{LI}P_r=N_0$. Therefore, we will take a step further than existing works [17, 18] and [19]. We compare the performance of TRSPA when applied to different relaying modes with reasonable SI suppression capabilities. Figure 4 compares the simulated outage performance of

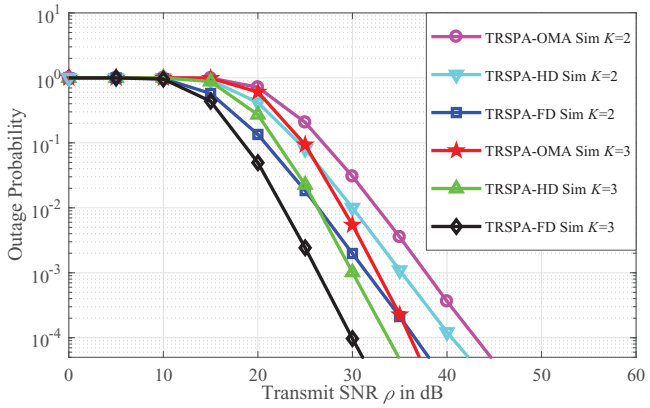

FIGURE 4 Simulated outage probabilities of D_2 versus transmit SNR for TRSPA-FD with reasonable SI suppression capabilities, TRSPA-HD and TRSPA-OMA with different relay numbers Ks under the hypothesis of H_1

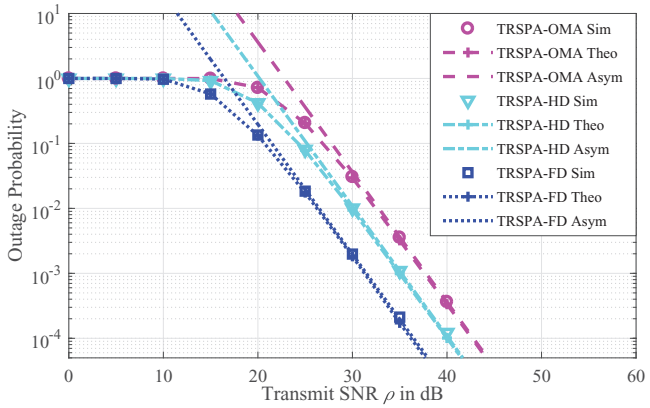

FIGURE 5 Simulated, exact and asymptotic outage probabilities of D_2 when $K = 2$ versus transmit SNR for TRSPA-FD with reasonable SI suppression capabilities, TRSPA-HD and TRSPA-OMA under the hypothesis of H_1

TRSPA-FD with TRSPA-HD and TRSPA-OMA in such case, while Figure 5 presents their simulated, exact and asymptotic values. Figure 4 illustrates the superior performance of TRSPA-FD in practical scenarios regardless of the SNR being high or low. The achieved diversity order of TRSPA-FD is equal to K in Figure 4, instead of zero. This observation verifies Remark 5 and is the most critical difference from Figures 2 and 3. Also, the outage performance of TRSPA-FD is not limited by any floor in practical scenarios. TRSPA-FD always achieves the best outage performance throughout the entire SNR range. Additionally, we learn that more relays lead to smaller outage probabilities due to higher diversity gains. Finally, the well-approximated curves in Figure 5 validate derivation results (20) (21) and (39).

Figure 6 presents the simulated ergodic rates of D_{1,k^*} for TRSPA-FD and other benchmarks versus transmit SNR under H_1. We assume that $R_2 = 0.1$ BPCU [4]. Their exact and asymptotic results are presented in Figure 7 which are obtained from (23), Corollary 2 and (29). Well-matched results validate these expressions. Using the two points (40 dB, 5.64BPCU) and (50 dB, 8.96BPCU) on the asymptotic curve of TRSPA-FD in Figure 7, we can compute the slope which is $3.32/10 = 0.332$.

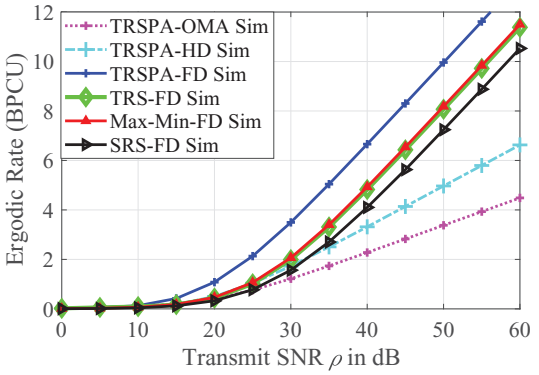

FIGURE 6 Simulated ergodic rates of D_{1,k^*} versus transmit SNR for TRSPA and benchmarks under the hypothesis of H_1

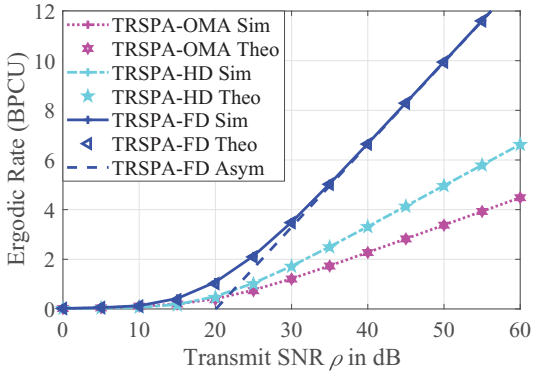

FIGURE 7 Simulated, exact and asymptotic ergodic rates of D_{1,k^*} versus transmit SNR for TRSPA and benchmarks under the hypothesis of H_1

The result verifies Remark 3 because $0.332 \times 10 \lg 2 = 1$. When it comes to the performance comparison, according to Figure 6, the proposed TRSPA-FD scheme achieves a larger ergodic rate for D_{1,k^*} compared with other RS strategies and relaying modes, because of i) its dynamic power allocation method, and ii) its feature of allowing D_{1,k^*} to transmit all the time. We know that D_{1,k^*} has to wait for its turn in TRSPA-HD and TRSPA-OMA schemes.

We present the simulated ergodic rate results under different numbers of relays for TRSPA-FD with reasonable SI suppression capabilities, TRSPA-HD and TRSPA-OMA in Figure 8. Figure 9 further presents their exact and asymptotic curves. In a similar method with Figure 7, the slopes of the ergodic rate curves in Figure 9 at the high SNR region for TRSPA-FD, TRSPA-HD and TRSPA-OMA are found to be 1, $\frac{1}{2}$, and $\frac{1}{3}$, respectively. The results verify Remark 3 and Remark 6. When it comes to performance comparison, we learn from Figure 8 that $K = 3$ achieves a larger ergodic rate than $K = 2$ due to a larger spatial diversity gain. It is observed that the ergodic rate of TRSPA-FD with reasonable SI suppression capabilities is larger than those of benchmarks due to simultaneously receiving and transmitting. However, there exists an exception. By careful observation on Figure 8, the ergodic rate of TRSPA-FD is found to be slightly exceeded by that of TRSPA-OMA when the

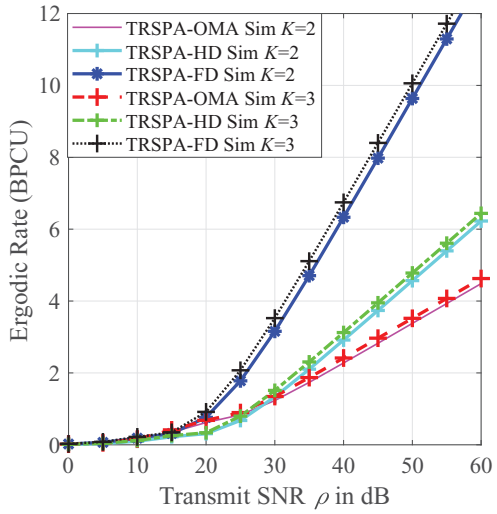

FIGURE 8 Simulated ergodic rates of D_{1,k^*} versus transmit SNR for TRSPA-FD with reasonable SI suppression capabilities, TRSPA-HD and TRSPA-OMA with different relay numbers Ks under the hypothesis of H_1

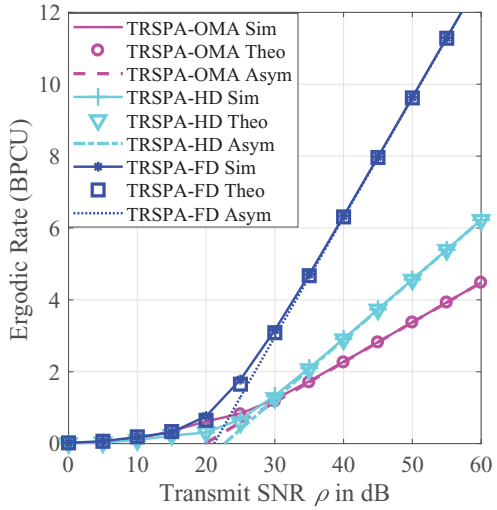

FIGURE 9 Simulated, exact and asymptotic ergodic rates of D_{1,k^*} when $K = 2$ versus transmit SNR for TRSPA-FD with reasonable SI suppression capabilities, TRSPA-HD and TRSPA-OMA under the hypothesis of H_1

transmit SNR is 15 dB. Such a phenomenon is already analyzed theoretically in Section 4. Based on Section 4, TRSPA-OMA's larger ergodic rate is obtained at the cost of worse outage performance. For the sake of practicality and fairness, we will further compare their achieved ergodic rates under the same outage performance requirement.

We compare TRSPA-FD with reasonable SI suppression capabilities, TRSPA-HD and TRDPA-OMA in Figures 10 and 11 under the same outage performance requirement P_{out}^{req}. Assume that $P_{out}^{req} = 0.001$ and $d_{D_2,BS} = 20$ m. As R_2 increases, the required transmit SNR by TRSPA-OMA is worked out based on (10) and Corollary 1 in a numerical method. Note that $P_{D_2}^{TRSPA-OMA} = P_{out}^{req}$ is used when working out that SNR value to guarantee the outage performance requirement. With

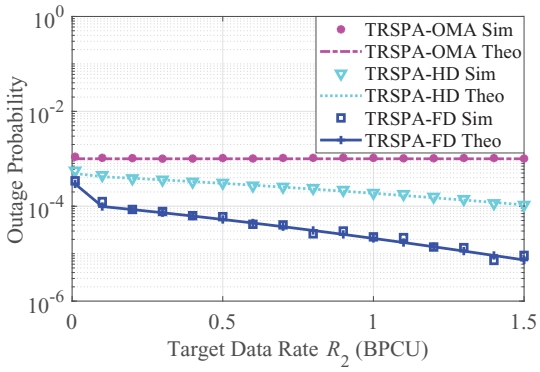

FIGURE 10 Simulated and exact outage probabilities of D_2 versus R_2 for TRSPA-FD with reasonable SI suppression capabilities, TRSPA-HD and TRSPA-OMA constrained by the predetermined outage performance requirement under the hypothesis of H_1

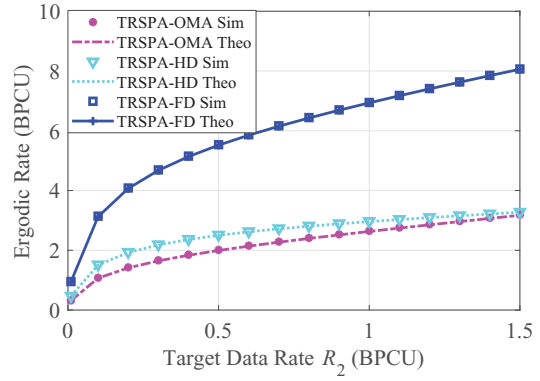

FIGURE 11 Simulated and exact ergodic rates of D_{1,k^*} versus R_2 for TRSPA-FD with reasonable SI suppression capabilities, TRSPA-HD and TRSPA-OMA constrained by the predetermined outage performance requirement under the hypothesis of H_1

the same SNR value for comparison fairness, we also plot the outage probability curves of TRSPA-FD and TRSPA-HD in Figure 10. As the x-axis increases from a small value, which implies that the transmit SNR rises from small as well according to (42), TRSPA-FD achieves the best outage performance. When R_2 continues to increase, TRSPA-FD continues to outperform other benchmarks. In summary, its outage probability is the lowest regardless of the SNR being large or small. It is shown in Figure 10 that the outage probabilities of all schemes are no larger than P_{out}^{req}. Therefore they indeed satisfy the preset QoS requirement, which is the premise of the ergodic rate comparison in Figure 11.

Under the outage probabilities shown in Figure 10, we compare the achieved ergodic rates of TRSPA-FD and benchmarks in Figure 11. When R_2 increases (i.e. the corresponding SNR increases) from a small value, TRSPA-FD achieves the largest ergodic rate compared with benchmarks. As R_2 keeps increasing, the ergodic rate of TRSPA-FD rises at a rate of 2, which is larger than those of TRSPA-HD and TRSPA-OMA. The observation verifies Remark 7. Therefore, TRSPA-FD always achieves the largest ergodic rate at all SNR values. Given the comparison results in Figure 10, we can conclude that

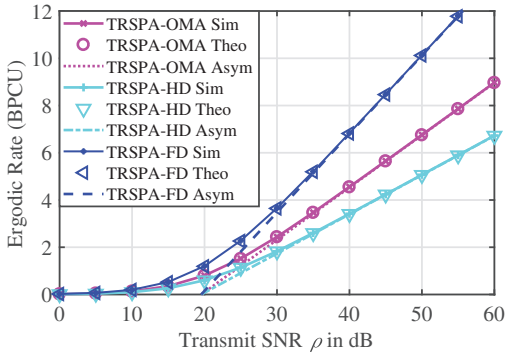

FIGURE 12 Simulated, exact and asymptotic ergodic rates of D_{1,k^*} versus transmit SNR for TRSPA-FD and various benchmarks under the hypothesis of H_0

TRSPA-FD always outperforms other benchmarks in terms of ergodic rate, regardless of the value of SNR, under the practical restriction of outage performance requirement.

Figure 12 shows the ergodic rates of D_{1,k^*} for TRSPA-FD and benchmarks under H_0. The exact and asymptotic values are worked out by (34)-(37). From Figure 12, we find that the slopes of ergodic rate curves for TRSPA-FD, TRSPA-HD and TRSPA-OMA in the high SNR region are respectively 1, $\frac{1}{2}$ and $\frac{2}{3}$. These values verify Remark 4. TRSPA-FD always obtains the largest ergodic rate under H_0 due to the benefit of using FD mode. Moreover, all RS strategies achieve larger ergodic rates under H_0 than H_1 (see Figure 8). It is because D_{1,k^*} transmits its signal using full power under H_0 but it allocates partial power to forward D_2's signal under H_1.

6 | CONCLUSION

This paper has proposed a power-allocation-based relay selection strategy TRSPA for FD-CNOMA with spectrum sensing, where "strong" user relays assist a "weak" user to transmit signals to the BS. Owing to optimal power allocations, TRSPA maximizes the ergodic rate of the selected relay on the condition of the weak user's successful transmissions. Uniform distribution has been employed for practically modelling the locations of relays. Exact and asymptotic expressions of outage probability and ergodic rate have been worked out. Accordingly, the diversity order is calculated to be zero, which means imperfectly cancelled LI severely restricts the outage performance. The spatial multiplexing gain is calculated to be one, which achieves its maximum achievable value. We then insightfully exploit the performance of TRSPA for FD-CNOMA with reasonable SI suppression capabilities, and compare it with TRSPA-HD and TRSPA-OMA. It is concluded that FD relaying mode is both outage optimal and ergodic-rate optimal for a practical TRSPA system. Finally, simulation results illustrate that our derivations are correct and that TRSPA is superior to other RS strategies including Max-Min, SRS and TRS. Even though LI impairs the advantages of the FD mode, current SI suppression techniques already enable TRSPA applied in the FD mode to achieve better performance than other relaying modes, that is TRSPA-HD and TRSPA-OMA.

ACKNOWLEDGEMENTS

This research was supported in part by National Natural Science Foundation of China (Grant No. 61771163), in part by the Natural Science Foundation for Outstanding Young Scholars of Heilongjiang Province (No. YQ2020F001), and in part by Science and Technology on Communication Networks Laboratory (No. SXX19641X072). The work of I. W.-H. Ho was supported in part by the General Research Fund (Project No. 15201118) established under the University Grant Committee of the Hong Kong Special Administrative Region, China, and in part by The Hong Kong Polytechnic University (Projects G-YBK6, G-YBR2).

CONFLICT OF INTEREST

No conflict of interest exits in the submission of this manuscript, and manuscript is approved by all authors for publication.

ORCID

Xinyu Wang https://orcid.org/0000-0001-6621-5598

REFERENCES

1. European Union, Identification and quantification of key socio-economic data to support strategic planning for the introduction of 5G in Europe-SMART 2014/0008, (2016)
2. Andrews, J.G., et al.: What will 5G be? IEEE J. Sel. Areas in Commun. 32(6), 1065–1082 (2014)
3. Mehaseb, M.A., et al.: Classification of LTE uplink scheduling techniques: an M2M perspective. IEEE Commun. Surveys Tutorials 18(2), 1310–1335 (2016)
4. Yue, X., et al.: Spatially random relay selection for full/half-duplex cooperative NOMA networks. IEEE Trans. Commun. 66(8), 3294–3308 (2018)
5. Ding, Z., et al.: A survey on non-orthogonal multiple access for 5G networks: research challenges and future trends. IEEE J. Sel. Areas Commun. 35(10), 2181–2195 (2017)
6. Wang, X., et al.: Full-duplex relaying cognitive radio network with cooperative nonorthogonal multiple access. IEEE Systems Journal 13(4), 3897–3908 (2019)
7. Ding, Z., Peng, M., Poor, H.V.: Cooperative non-orthogonal multiple access in 5G systems. IEEE Commun. Lett. 19(8), 1462–1465 (2015)
8. Men, J., Ge, J.: Performance analysis of non-orthogonal multiple access in downlink cooperative network. IET Commun. 9(18), 2267–2273 (2015)
9. Cover, T.: Broadcast channels. IEEE Trans. Inf. Theory 18(1), 2–14 (1972)
10. Tehrani, P., Lahouti, F., Zorzi, M.: Resource allocation in OFDMA networks with half-duplex and imperfect full-duplex users. In: IEEE International Conference on Communications (ICC), Kuala Lumpur, (2016)
11. Ding, Z., Dai, H., Poor, H.V.: Relay selection for cooperative NOMA. IEEE Wireless Commun. Lett. 5(4), 416–419 (2016)
12. Yang, Z., et al.: Novel relay selection strategies for cooperative NOMA. IEEE Trans. Veh. Technol. 66(11), 10114–10123 (2017)
13. Lv, L., et al.: Design of cooperative non-orthogonal multicast cognitive multiple access for 5G systems: user scheduling and performance analysis. IEEE Trans. Commun. 65(6), 2641–2656 (2017)
14. Xu, P., et al.: Optimal relay selection schemes for cooperative NOMA. IEEE Trans. Veh. Technol. 67(8), 7851–7855 (2018)
15. Laneman, J.N., Tse, D.N.C., Wornell, G.W.: Cooperative diversity in wireless networks: efficient protocols and outage behavior. IEEE Trans. Inf. Theory 50(12), 3062–3080 (2004)

16. Riihonen, T., Werner, S., Wichman, R.: Optimized gain control for single-frequency relaying with loop interference. IEEE Trans. Wireless Commun. 8(6), 2801–2806 (2009)
17. Yue, X., et al.: Exploiting full/half-duplex user relaying in NOMA systems. IEEE Trans. Commun. 66(2), 560–575 (2018)
18. Wang, X., et al.: Exploiting full-duplex two-way relay cooperative non-orthogonal multiple access. IEEE Trans. Commun. 67(4), 2716–2729 (2019)
19. Yue, X. et al.: Outage performance of full/half-duplex user relaying in NOMA systems. IEEE International Conference on Communications (ICC), Paris (2017)
20. Zhang, L., Liang, Y.-C., Xiao, M.: Spectrum sharing for internet of things: a survey. IEEE Wireless Commun. 26(3), 132–139 (2019)
21. Zhang, L., et al.: Performance analysis and optimization in downlink NOMA systems with cooperative full-duplex relaying. IEEE J. Sel. Areas Commun. 35(10), 2398–2412 (2017)
22. Zhou, Y., Wong, V.W.S., Schober, R.: Stable throughput regions of opportunistic NOMA and cooperative NOMA with full-duplex relaying. IEEE Trans. Wireless Commun. 17(8), 5059–5075 (2018)
23. Xu, B. et al.: Outage performance of downlink full-duplex network-coded cooperative NOMA. IEEE Wireless Commun. Lett. 1–1, (2020)
24. Tregancini, A., et al.: Performance analysis of full-duplex relay-aided NOMA systems using partial relay selection. IEEE Trans. Veh. Technol. 69(1), 622–635 (2020)
25. Guo, C., et al.: Energy harvesting enabled NOMA systems with full-duplex relaying. IEEE Trans. Veh. Technol. 68(7), 7179–7183 (2019)
26. Lima, B.K.S., et al.: Adaptive power factor allocation for cooperative full-duplex NOMA systems with imperfect SIC and rate fairness. IEEE Trans. Veh. Technol. 69(11), 14061–14066 (2020)
27. Ahmed, M.A., Baz, A., Tsimenidis, C.C.: Performance analysis of NOMA systems over Rayleigh fading channels with successive-interference cancellation. IET Commun. 14(6), 1065–1072 (2020)
28. Rodriguez, L.J., Tran, N.H., Le-Ngoc, T.: Performance of full-duplex AF relaying in the presence of residual self-interference. IEEE J. Sel. Areas in Commun. 32(9), 1752–1764 (2014)
29. Tabassum, H., Hamdi, A., Hossain, E.: Analysis of massive MIMO-enabled downlink wireless backhauling for full-duplex small cells. IEEE Trans. Commun. 64(6), 2354–2369 (2016)
30. Jing, Y., Jafarkhani, H.: Single and multiple relay selection schemes and their achievable diversity orders. IEEE Trans. Wireless Commun. 8(3), 1414–1423 (2009)
31. Jia, M., et al.: Performance analysis of cooperative non-orthogonal multiple access based on spectrum sensing. IEEE Trans. Veh. Technol. 68(7), 6855–6866 (2019)
32. Abramowitz, M., Stegun, I.A.: Handbook of Mathematical Functions with Formulas, Graphs, and Mathematical Tables. Dover, Washington, DC (1964)
33. Hossain, M.J., Alouini, M.-S., Bhargava, V.K.: Multi-user opportunistic scheduling using power controlled hierarchical constellations. IEEE Trans. Wireless Commun. 6(5), 1581–1586 (2007)
34. Gradshteyn, I.S., Ryzhik, I.M.: Table of Integrals, Series and Products, 6th ed., Academic, New York (2000)
35. Lee, J., Jindal, N.: High SNR analysis for MIMO broadcast channels: dirty paper coding versus linear precoding. IEEE Trans. Inf. Theory 53(12), 4787–4792 (2007)
36. Wang, L., et al.: Secure transmission with antenna selection in MIMO nakagami-m fading channels. IEEE Trans. Wireless Commun. 13(11), 6054–6067 (2014)

How to cite this article: Wang X, Jia M, Ho Ivan Wang-Hei, Guo Q, Lau Francis Chung-Ming. Relay selection for spatially random full-duplex cooperative non-orthogonal multiple access networks. *IET Commun.* 2021;15:1060–1075.
https://doi.org/10.1049/cmu2.12142